Analytical/Experimental Comparison of the Axial Velocity in Trailing Vortices

M. Giuni*

University of Glasgow, Glasgow G12 8QQ, Scotland, UK

E. Benard†

Institut Supérieur de l'Aéronautique et de l'Espace, 31055 Toulouse, FRANCE

The axial velocity of a vortex is a parameter which is known to be strongly related to the vortex breakdown, yet to date a complete description of its physical origins has not been achieved. A series of experiments studying the vortex trailed from a NACA 0015 wing using stereoscopic particle image velocimetry is presented and the axial velocity studied in detail. The problem of centering the instantaneous vector fields is addressed showing a high sensitivity of the results from the centering method which is adopted. It is shown that a strong axial velocity excess exists and a linear relationship between the axial velocity and a circulation parameter of the vortex is shown. The experimental data are compared with the analytical descriptions of the velocity in the centre of a simplified vortex giving new insights of the viscous effects in the development of the axial flow.

Nomenclature

ΔH	Batchelor dissipation function, m^2s^{-2}	c	Wing chord, m
Γ	Overall Circulation, m^2s^{-1}	r	Radial coordinate, m
$\tilde{\Gamma}$	Circulation profile as function of the radius, m^2s^{-1}	Re	Reynolds number
AoA	Angle of attack, deg	U_∞	Freestream velocity, ms^{-1}
AR	Wing aspect ratio	v_t	Swirl velocity, ms^{-1}
b	Wing semi-span, m	w	Axial velocity, ms^{-1}
		w_0	Axial velocity in the vortex centre, ms^{-1}
		x	Spanwise coordinate, m
		y	Vertical upwards coordinate, m
		z	Streamwise coordinate, m

I. Introduction

Wing tip vortices have been studied many times during the last four decades. However, to date a full understanding of the relationship between the numerous salient flow features has not been achieved. Cross boundary layer separation, vorticity sheet rolling up, secondary vortices, vortex instability are known to be important physical mechanisms which contribute to the vortex formation, yet the process is still poorly understood.

Controlling the wing tip vortices is of importance in many practical engineering problems. For instance, the blade-vortex interactions noise radiated from helicopter blades and the hazards created by the presence of vortices trailed from aircraft wings are both directly effected by the vortex formation mechanism. One of the main purposes of the research in wing tip vortices is therefore to reduce the effects of the vortex, and to accelerate its decay.

Vortex flows are characterized by the large swirl velocity, however there also exists an axial velocity at the core of the vortex, which flows perpendicular to the swirl velocity. Unlike the swirl velocity, the effects

*PhD Student, Department of Aerospace Engineering, AIAA Student Member.

†Senior Lecturer, Department of Aerodynamics, Energetics and Propulsion.

of the axial flow are subtle. Though the axial velocity deficit/excess can be smaller in comparison to swirl velocity, its presence dictates to a large extent the stability and decay of the vortex and it is known to be a significant parameter in the breakdown of the vortex.[1] The axial flow has been intensively studied throughout the years and has been shown to either be directed towards the airplane (wake-like, as behind a nonlifting drag-producing body) or away from it (jet-like). It is known to be dependent on several factors: wing geometry, angle of attack, Reynolds number, wing boundary layer, and turbulence dissipation in the vortex core.[2] To date, there is still no established theory which can reliably predict the magnitude or even the direction of this axial velocity for simple tip vortex flow. Furthermore, the physical mechanism of how this axial flow forms is still poorly understood.

In 1964 Batchelor[3] proposed an analytical description of the axial flow inside an idealized vortex and the following result was derived:

$$w_0^2 = U_\infty^2 + \int_r^\infty \frac{1}{4\pi^2 r^2} \frac{\partial \tilde{\Gamma}^2}{\partial r}\, dr - 2\Delta H \tag{1}$$

with w_0 the axial velocity in the vortex centre, U_∞ the freestream velocity, r the radial cylindrical coordinate, $\tilde{\Gamma}$ the circulation profile across the vortex and ΔH an arbitrary function added to account the dissipation along a streamline passing through a viscous region of the flow (for example, the boundary layer shed from the wing trailing edge and rolling around the tip vortex). This result was obtained by steady axisymmetric cylindrical incompressible Navier–Stokes equations with the assumption of small axial gradients compared with the radial gradients and small radial velocity compared to axial and swirl velocity (boundary layer type approximation). With assumptions of constant dissipation term and vortex radius, Eq. (1) shows an increase of axial velocity with an increase of overall circulation and a velocity excess in inviscid fluids where $\Delta H = 0$. The presence of viscous losses competes with the inviscid acceleration mechanism.

Another step in the analytical description of a vortex is signed by Moore and Saffman[4] who have arrived to a more complex equation for the axial flow in laminar trailing vortices taking into account also of the boundary layer shed by the wing and entrained in the core. In this way they remove the singularity in the origin that is present in Eq. (1).

The fact that experiments show either an excess or a deficit in the axial velocity was quantified in 1998 by Spalart[5] where an explanation of the vortex centre axial velocity was introduced in two mathematically equivalent ways: from considerations of the helical shape of vortex lines and from equating the pressure from different points of the vortex. Both the descriptions leads to the following equation which can be also seen as the radial differentiation of Eq. (1) when the term with ΔH is ignored:

$$\frac{d(w^2 + v_t^2)}{dr} + 2\frac{v_t^2}{r} = 0 \tag{2}$$

where v_t is the tangential velocity. Because the circulation profile can be expressed as $\tilde{\Gamma} = 2\pi r v_t$, Eq. (2) can be rewritten as

$$4\pi^2 r^2 \frac{d\, w^2}{dr} + 2\frac{d\, \tilde{\Gamma}^2}{dr} = 0 \tag{3}$$

Because it is generally observed that $\tilde{\Gamma}$ increases with r, it is clear that w increases as the vortex axis is approached (jet-like axial flow). It is then provided the nondimensional circulation parameter $\Gamma/U_\infty b$ as the key parameter for axial velocity excess or deficit, where Γ is now the overall vortex circulation and b the wing semi-span. Large values of the circulation parameter result in an excess and low values in a deficit of axial velocity. For example, Chow et al.[6] show an axial velocity of $1.78U_\infty$ with a circulation parameter of 0.20 and, in contrast, Devenport et al.[7] report an axial velocity of $0.85U_\infty$ corresponding to a circulation parameter of 0.028. This low value of the circulation parameter suggests that the viscous effects in this case overcome the inviscid accelerating mechanism. Anderson et al.[8] have recently (2003) presented a wide range of tests where experimental axial velocity measurements show a linear relation between the circulation parameter and the axial velocity.

The work presented here focuses on the study of the axial velocity of a wingtip vortex. The experiments involve Stereocopic Particle Image Velocimetry method to study the velocity field of a tip vortex. PIV techniques respect global and non-intrusive criteria which are required for a vortex experimental study.[2] After a discussion on the centering of the instantaneous vector fields, the axial velocity peaks are plotted against the circulation parameter along with the results from other works. Lastly, an evaluation of the correctness of the analytical descriptions in describing these experiments is presented and the viscous losses term ΔH is further discussed.

II. Experimental Arrangement and Procedure

The experiments were conducted at the University of Glasgow in the low-speed "Argyll" wind tunnel, a closed-return facility with test section dimensions 2.65 m wide by 2.04 m high by 5.60 m. The model was a NACA 0015 wing with 0.42 m chord, 1.4 m span and rectangular wing tip (see Fig. 1(a)) allowing tests with small wall interference and blockage effects. The model was mounted on a plate outside the test section where height and angle of attack adjustments were set. The wing was positioned in the middle height of the test section with the tip along the centerline.

The reference system origin was on the wing tip trailing edge with x as spanwise coordinate, y vertically directed upwards and z coordinate along the freestream direction.

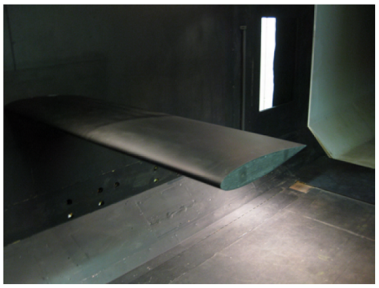

(a) Model and test chamber.

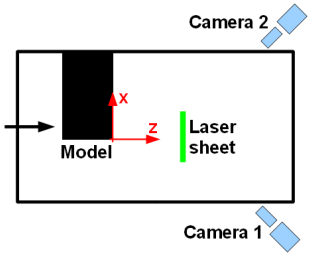

(b) Cameras and laser.

Figure 1. Experimental arrangement.

Two CCD cameras of 11 Mpixels were mounted on the sides of the test section independently from the wind tunnel (see Fig. 1(b)); 300 mm Nikon lenses were used and the f-number was 8. Angular stereoscopic system in Scheimpflug condition, as described by Zang and Prasad,[9] were adopted with angles between the camera and the object plane of around 35°. This value maintains low errors in the evaluation of both the in-plane and out-of-plane velocity component.[10] A double-frame/single-pulse method[11] was used so that for each time step two images were recorded for each camera corresponding to the two different laser pulses. The light source of the laser sheet was provided by a dual cavity Nd:YAG laser with 532 nm wavelength. A laser guiding arm was installed on a rail placed above the test section that allowed two-dimensional translations and three axes rotations of the laser. The laser sheet, of 3 mm of thickness, passed through a window on the top of the test section. The calibration of the cameras, the image acquisition, the laser control and the cross-correlation were accomplished by the LaVision software DaVis 7.2. A dual-plane calibration plate of 300 mm by 300 mm was used; the field of view of the cameras was of the same order. Every time the laser sheet was moved, a new adjustment of cameras (angles and separation) and a new calibration was performed.

A stereo cross-correlation of the image pairs were accomplished by a double step process on an interrogation window of 64 by 64 pixels with 25% of overlap followed by other two steps with interrogation window of 32 by 32 pixels with 50% of overlap leading to the calculation of 53300 vectors per frame and 1.2 mm of vector spatial resolution as documented by Giuni et al.[12] The processed data were stored in an external hard disk of 1.5 TBytes.

The flow was seeded with olive oil particles by an Aerosol Generator PivPart40 serie installed at the end of the test section. The peak in the probability density function of the olive oil particles size distribution was at 1 μm that corresponds, following the procedure described by Adrian,[13] to a particle diameter between 1 and 2 pixels which is what suggested by Prasad et al.[14] to reduce peak-locking effects and to ensure a good quality in the correlation.

The wingtip vortex has been studied for Reynolds numbers of $1 \cdot 10^5$, $5 \cdot 10^5$ and $10 \cdot 10^5$ and angles of attack of the wing of 4°, 8°, 12° and 15° at planes perpendicular to the freestream at $z/c = 0.25$, 0.5, 1 and 2 from the trailing edge. Each test consisted in the acquisition of sets composed by 121 two images pairs at a constant frequency of 2 Hz.

III. Results and Discussion

A. Centering

The problem of the wandering of the vortex has been well acknowledged although the reasons are a combination of freestream turbulence, wind tunnel walls effects, unsteadiness arising from the model and multiple vortices. Various procedures have been developed to correct vortex flow measurements from the resulting biasing effects. For one-point measurements, Devenport et al.[7] proposed a mathematical description of the wandering effects, the results of which provide methods for determining the amplitude of wandering

and reversing those effects. For global measurements, such as PIV, the basic idea of all the methods is to re-collocate the centre of the tip vortex in each of the instantaneous velocity measurements frames before averaging.[15] The challenge therefore is in identifying a unique property of the vortex which can be used to define its centre. Different methods have been used and studied, and Ramasamy et al.[15] compared the uncorrected measures of the turbulence inside a helicopter blade wingtip vortex with five vortex centre detection methods: centroid of vorticity, peak axial velocity, helicity minimum, zero in-plane velocity and Q-criterion defined as the discriminant of a particular velocity gradient tensor. Clearly, for axisymetric and fully developed vortex, the centres identified by all the different methods are exactly in the same position. It was found that the method that best describes both the in-plane and out-of-plane quantities is the helicity aperiodicity correction because it includes all the velocity components in its calculation (cross product of out-of-plane vorticity and axial velocity). In their cases the vortex centre axial velocity was always detected as a deficit.

Depending on which quantity and aspect of the vortex is of interest, the vortex centre detection method can significantly effects the results. In order to visualize and quantify the wandering of the vortex, Fig. 2(a) is a plot of the 121 instantaneous vortex centres of 121 samples as detected using four centering methods: vorticity minimum, cross velocity maximum, helicity minimum and zero in-plane velocity. A different scattering of the centres is observed with a standard deviation around two percent of the chord. Although the centre time history is different for each detection method, the average positions are clustered as seen in Fig. 2(b).

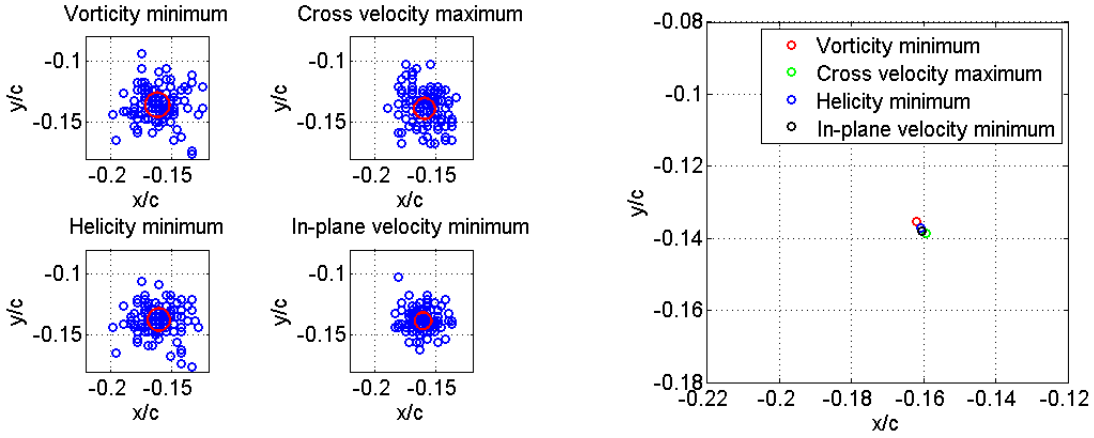

(a) Instantaneous centres.

(b) Averaged centres.

Figure 2. Vortex centres evaluated with different centering methods for $z/c = 0.5$, $Re = 1 \cdot 10^5$, $AoA = 15°$.

The axial velocity profiles of two sample cases are plotted in Fig. 3 in order to illustrate the effect of the vortex centering method. Cuts every 30 degrees around the vortex centre, have been made and the averaged velocity profiles along these radius are plotted. The red curves represent the average of the 12 profiles. The average from three different centering methods are presented: no correction, maximum axial velocity and minimum helicity. The vorticity needed for the evaluation of the helicity has been calculated with the circulation method as presented by Raffel.[16] It is observed that there is a large change of the magnitude and distribution of the axial velocity profiles with the choice of the centering method. As expected, the axial velocity centering method shows a higher maximum axial velocity peak in the vortex centre than the other methods. It is also noted in Fig. 3(f) that the helicity centered vortex has not the maximum axial velocity in the centre. Furthermore, at low angles of attack, the axial velocity vortex detection method shows a small excess in the centre while the other methods see a deficit. At one chord of distance from the trailing edge the difference is still significant.

This particular aspect has been explained by Giuni et al.[17] in relation to the peculiar structure of the vortex near field at low angles of attack. The vortex core appears as an island of low velocity with subregions of comparable excess and deficit velocity which rotate within the core. This leads to a non-unique axial velocity peaks and a strong dependency on the searching technique. At the contrary, at high angles of attack, the peak (velocity excess) is well defined and much more intense than the velocity deficit regions around it. The use of the axial velocity method is therefore preferable when the study is focused on

the axial velocity itself with the limit of questionable results at low angles of attack. This method leads to higher and more defined peaks due to the fact that the vortex is always translated so that the maximum velocity is in the centre.

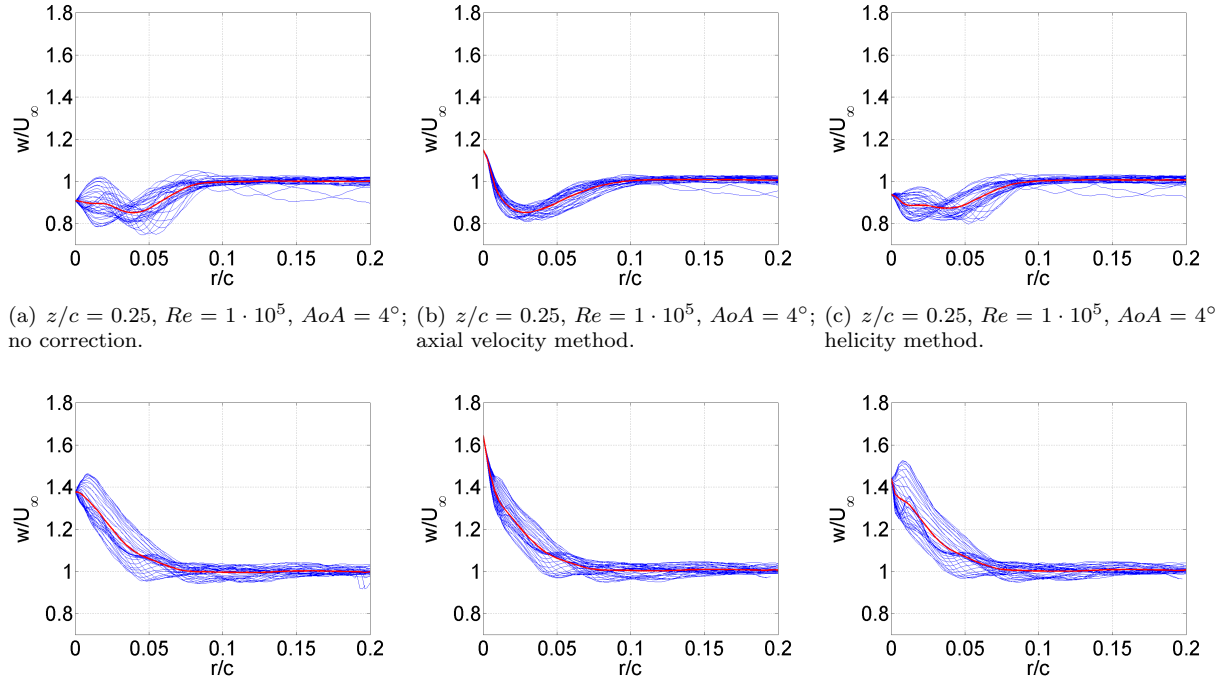

(a) $z/c = 0.25$, $Re = 1 \cdot 10^5$, $AoA = 4°$; no correction. (b) $z/c = 0.25$, $Re = 1 \cdot 10^5$, $AoA = 4°$; axial velocity method. (c) $z/c = 0.25$, $Re = 1 \cdot 10^5$, $AoA = 4°$; helicity method.

(d) $z/c = 1$, $Re = 10 \cdot 10^5$, $AoA = 12°$; no correction. (e) $z/c = 1$, $Re = 10 \cdot 10^5$, $AoA = 12°$; axial velocity method. (f) $z/c = 1$, $Re = 10 \cdot 10^5$, $AoA = 12°$; helicity method.

Figure 3. Axial velocity profiles.

The importance in clearly identifying and defining an aperiodic correction method and how the particular feature which is to be studied determines this choice have been highlighted . Therefore, it is not really possible to say that there is a definite method for the vortex centre detection, but different method are suited to different measurements, especially in the near field where the vortex is not well developed yet. Furthermore, different results in comparing with other experiments need to be done considering also the different centering methods applied. The axial velocity aperiodicity correction method is then used in the following sections.

B. Axial Velocity Peak

The averaged axial velocity profiles are reported in relation of the change in wake position (Fig. 4(a)) and in angle of attack (Fig. 4(b)). It appears a decrease of the peak axial velocity by approximately 10% as it convects downstream from $0.25c$ to $2c$ and an increase with the angle of attack from w_0/U_∞ of 1.1 to 1.7. The small difference in the peak between 12° and 15° is due to the fact that the wing is working in a region close to the stall angle.

B.1. Velocity peaks

The axial velocity peaks of all the tests against angle of attack are presented in Fig. 5. There is a clear linear relationship between the angle of attack and the axial velocity in the range studied. At Reynolds number of 100,000 and angle of attack of 15 degrees, a decrease of axial velocity is recorded probably related to an initial stall of the wing. In general, the larger angles of attack show a greater scatter of axial velocity peaks.

A typical circulation profile obtained by integrations of the tangential velocity is presented in Fig. 6. An initial linear trend of the circulation against the radius is observed up to a radius approximately equal to the vortex core size (radius at which the maximum tangential velocity is observed). There is then a small but constant increase of the circulation, due to the fact that the vortex is not yet fully developed in the early wake.

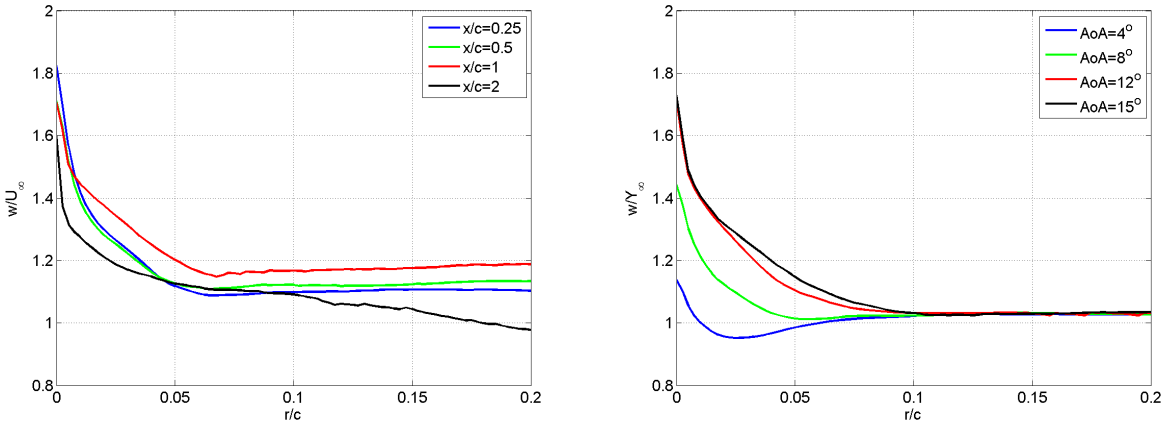

(a) As function of the position for $Re = 1 \cdot 10^5$, $AoA = 15°$. (b) As function of the angle of attack for $z/c = 1$, $Re = 5 \cdot 10^5$.

Figure 4. Axial velocity profile.

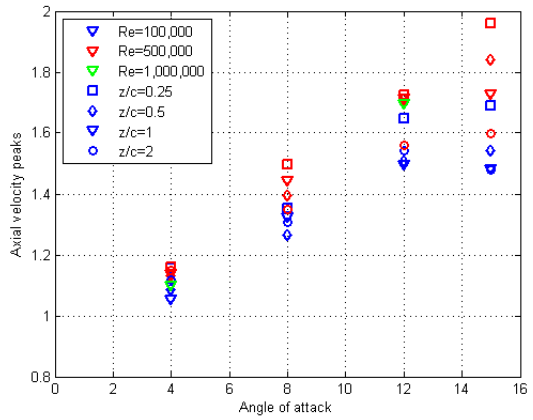

Figure 5. Axial velocity peaks as a function of angle of attack.

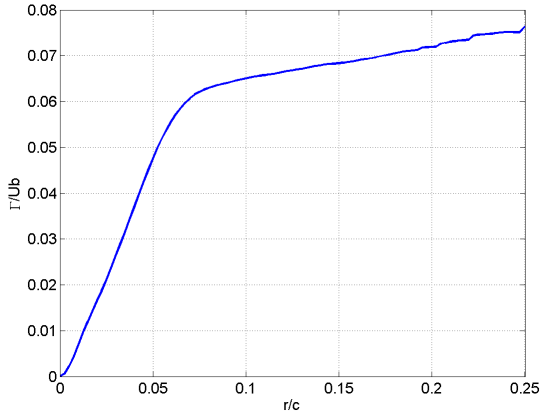

Figure 6. Vortex circulation for $z/c = 1$, $Re = 5 \cdot 10^5$, $AoA = 8°$.

The circulation parameter $\Gamma/U_\infty b$ against the angle of attack is plotted in Fig. 7 and the axial velocity peaks as function of the circulation parameter are plotted in Fig. 8 where the overall circulation has been evaluated at radius $r/c = 0.24$. A linear trend is observed in both the plots although a high scatter of the data is also observed.

B.2. Data comparison and new circulation parameter

The experimental results presented in the previous section are compared with the data from Anderson and Lawton experiments.[8] They tested a NACA 0015 section wing model with 0.762 m of chord and an aspect ratio of 0.8. The study focused on the axial velocity in the vortex core and its dependence on the Reynolds number (750,000, 1,000,000 and 1,250,000), tip shape (flat and rounded), angle of attack (4°, 6°, 8° and 10°) and wake plane location (1 and 2 chords downstream from the trailing edge). The point measurements were obtained using a triple-sensor hot-wire probe.

Their results are compared with the current study. In particular, the relations between circulation, angle of attack and axial velocity are studied.

Circulation parameter and angle of attack. Anderson et al.[8] noted a linear relationship between the angle of attack and the circulation parameter. These results are compared with the present experimental study in Fig. 9(a). The same linear trend is noted also in the present work but a different slope is seen. The difference between the curves can be attributed to the different wing area and lift produced.

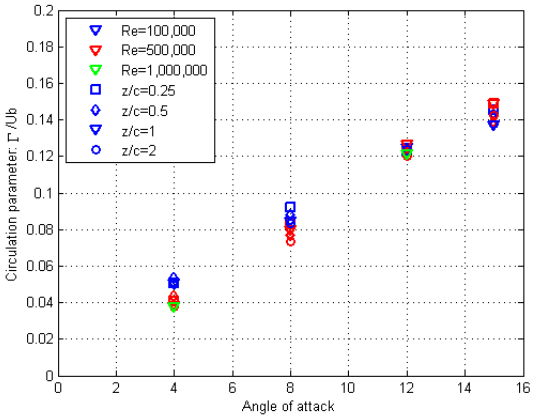

Figure 7. Circulation parameter as a function of angle of attack ($r/c = 0.24$).

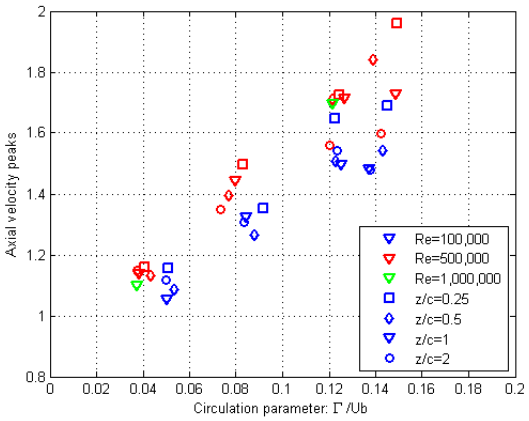

Figure 8. Axial velocity peaks as a function of circulation parameter.

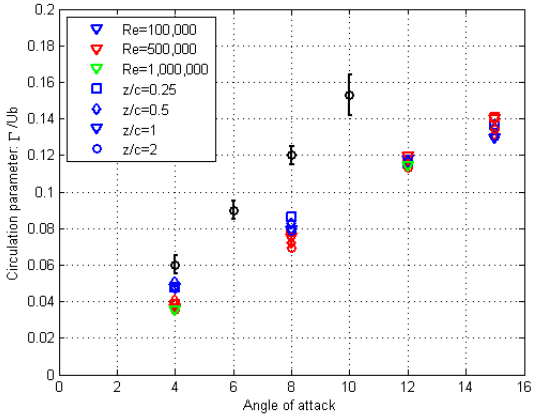

(a) Comparison circulation parameter as a function of angle of attack.

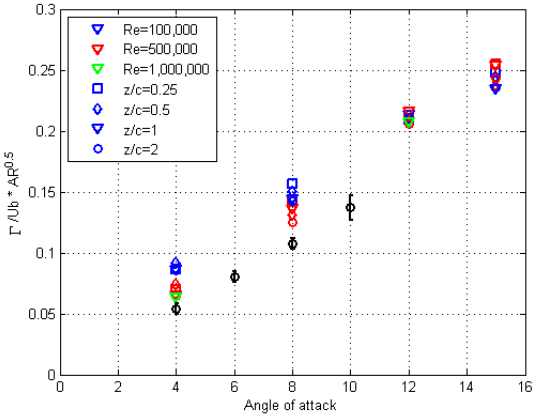

(b) Comparison aspect ratio modified circulation parameter as a function of angle of attack.

Figure 9. Circulation parameter and angle of attack.

A new circulation parameter which account for the wing aspect ratio is then proposed:

$$\Gamma_S = \Gamma / U_\infty b \cdot AR^{0.5} \tag{4}$$

This new circulation parameter is plotted in Fig. 9(b) against the angle of attack and a good agreement of the two experimental results is observed. Further studies on the reasonability of these parameters and a derivation from theoretical analysis are in progress.

Circulation parameter and axial velocity. Anderson et al.[8] had already shown the linear trend between the axial velocity peak and the circulation parameter. More experimental results are here reported for a comparison with the current study. The characteristic parameters of these experiments are shown in Table 1.

The various experiments are compared in Fig. 10(a) where the axial velocity peaks are plotted against the circulation parameter. It appears a linear relationship between the circulation parameter and the axial peaks, however a significant scatter between the different experiments is observed.

Table 1 shows a range of aspect ratios in the experiments from 0.75 to 4.3, suggesting a dependence on this parameter. Furthermore, the circulation parameter as currently defined misses any chord dependency.

The new circulation parameter defined in Eq. (4) is used to plot the different experiments results in if Fig. 10(b). A linear relationship between the results with less scatter then what observed in Fig. 10(a)

Experiments	Re	AR	Airfoil	Tip geometry
Devenport et al.[7]	$5.3{\cdot}10^5$	4.3	NACA 0012	flat
Green[2]	$6.8{\cdot}10^5$	2.3	NACA 64309	round
Chow et al.,[6] Dacles et al.[18]	$4.6{\cdot}10^6$	0.75	NACA 0012	round

Table 1. Experiments comparison.

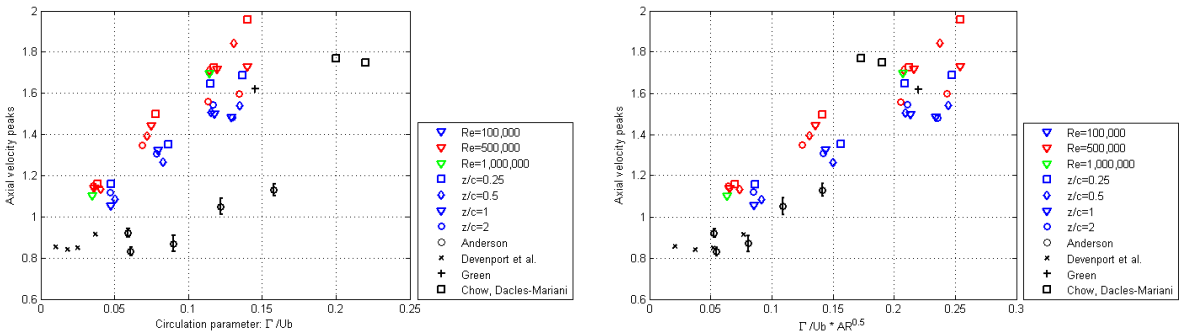

(a) Comparison axial velocity near the centre of the vortex as a function of the circulation parameter.

(b) Comparison axial velocity near the centre of the vortex as a function of the aspect ratio modified circulation parameter.

Figure 10. Circulation parameter and axial velocity.

is observed. It is furthermore noted that the circulation parameter in the present tests was too high to show an axial velocity deficit or, in another way, the inviscid accelerating mechanism was stronger than the decelerating viscous effects.

C. Comparison with analytical vortices

Eq. (3) links the square axial velocity gradient multiplied by the square distance from the centre with the square circulation gradient and a dimensionless form of the equation can be obtained using the chord and the freestream velocity. The two terms of the equation have then been evaluated from the axial velocity and circulation (i.e. tangential velocity integral) profiles and plotted in dimensionless form in Fig. 11 as function of the radius.

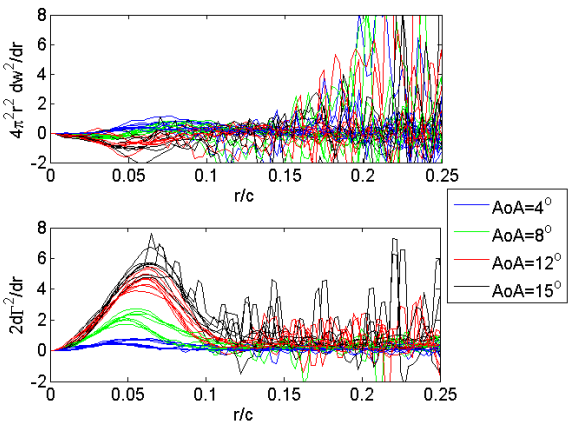

Figure 11. Circulation and axial velocity gradients terms.

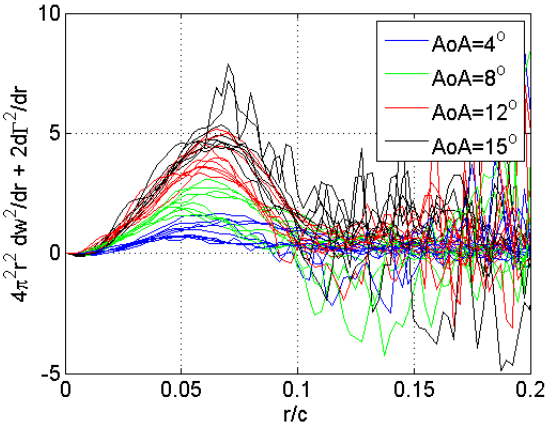

Figure 12. Error in gradients equation.

High noise is observed at the edges of the vortex where the tendency to an asymptotic zero value is also observed. Both the terms are equal to zero at the vortex centre and find a peak at a distance from the centre at the order of the vortex core dimension. It appears as well that the circulation term has higher

values then the axial term (the axial velocity term has been plotted with a minus in order to make easier the comparison). The sum of the who terms is then plotted in Fig. 12 which can be seen as the error of the equation or as the distance of the experiment from that analytical description. It is clear how the assumptions taken to derive the Eq. (3) are not valid for these cases: it is a flow far from be laminar and the losses from the boundary layer which rolls up around the vortex is not taken into account. Furthermore, the clustering of the curves for same angle of attack suggests a dependency between the error and the overall vortex circulation.

Eq. 1 describes the vortex centre axial velocity including a viscous losses term ΔH not more specified. Although that equation is commonly accepted, as far as the authors concern there have been no attempts to prove its applicability and correctness against experimental data and a further discussion on the losses term is not present in literature. This equation, as also Eq. (3), is based on laminar flow and inviscid fluid. If the losses term ΔH is taken as a comprehensive value of all the terms not included in the equation derivation, basic considerations on the losses (e.g turbulent dissipation, boundary layer) can be done.

The integration in Eq. 1 has been computed with the experimental data of the circulation and the axial velocity peak is then calculated. In Fig. 13, the dimensionless form of the measured axial velocity peaks are plotted on the left hand side as function of the angle of attack; on the right hand side, the axial velocity peaks estimated from Eq. (1) are plotted when the losses term is ignored. The difference between the two plots is then directly linked to term ΔH.

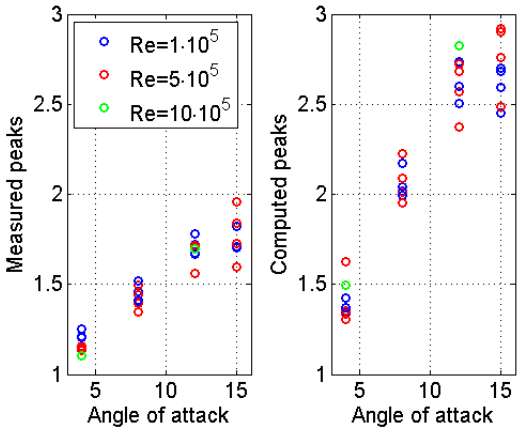

Figure 13. Measured axial velocity peaks and evaluation without losses.

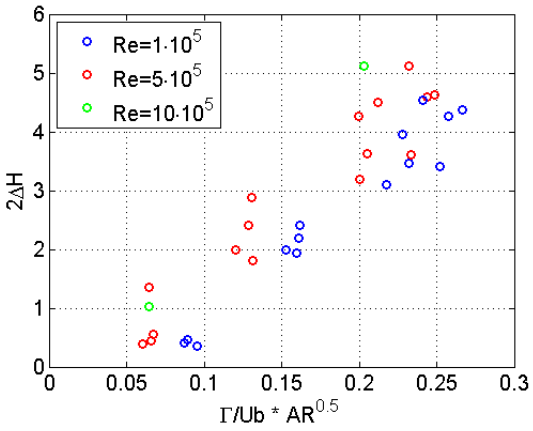

Figure 14. Axial velocity peaks and evaluation without losses.

When the losses are neglected (right hand side), the analytical results give a higher axial velocity excess reaching almost a value of 3 times the freestream velocity. As expected, an increase in the peak with the angle of attack is observed because directly dependent on the circulation.

In Fig. 14 the dimensionless viscous losses term is plotted as function of the new circulation parameter introduced in the previous section. Even though a high dispersion is detected, a linear trend is observed and a weak Reynolds number effect is visible with a higher value of the dissipation term for a higher Reynolds number.

Lastly, in Fig. 15(a) the losses term ΔH scaled by the circulation parameter $\Gamma/U_\infty b \cdot AR^{0.5}$ is plotted against the angle of attack. It appears that the losses so scaled are independent from the angle of attack at the exception of lower values at 4 degrees. As mentioned earlier and discussed more by Giuni,[17] the cross velocity maximum centering method is not fully reliable where the axial velocity peaks are not well defined (i.e. low angle of attack). In Fig. 15(b) the same losses term has been evaluated when the helicity minimum centering is adopted. Higher losses term are computed and comparable values between the angles of attack is observed.

The Reynolds number effect in these plots is also very clear. Although the increase of the Reynolds number corresponds to an increase of the inertia on to the viscous effects, for a higher Reynolds number appears a higher scaled losses term that is a higher distance between the measured axial velocity peak and what the analytical description calculates. It is then observed that the decelerating viscous effects grows faster than the accelerating inviscid mechanism. It is believed that the turbulence inside the vortex is one of the main causes of this behaviour and studies on this area are in progress.

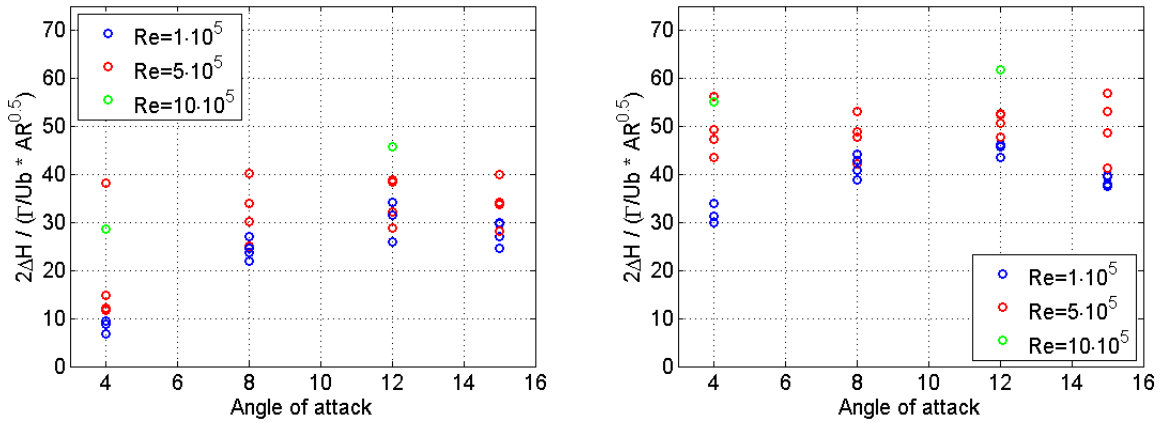

(a) Cross velocity maximum correction method.

(b) Helicity minimum centering method.

Figure 15. Losses term scaled with the centering parameter.

IV. Conclusion

The axial velocity in the near field of a wing trailing vortex has been investigated with a Stereoscopic Particle Image Velocimetry. Because the vortex moves around, the instantaneous vector fields need to be centered before the average can be taken. It has been shown that the centering method strongly affects the results and that the choice is not unique but depends on which particular aspect is of interest.

When the cross velocity peak centering method is adopted, the averaged axial velocity in the vortex centre is always measured as an excess in reference to the freestream velocity and it increases with the angle of attack. A circulation parameter which takes into account of the wing aspect ratio has been proposed and a linear relationship with the velocity peak has been observed. A good agreement with previous results has also been observed.

A comparison with laminar analytical vortices in inviscid flows has shown the limit of these descriptions when the vortex is turbulent and not yet fully developed. The losses term ΔH introduced by Batchelor[3] which takes into account of the viscous decelerating mechanism has been studied in more detail. When scaled with the circulation parameter, this term is independent from the angle of attack and a Reynolds number effect stands out.

The different aspects concerning the formation mechanism and prediction of the axial velocity behaviour in wing trailing vortices are not clear and further studies on this topic are needed. In particular, the turbulence inside the vortex is believed to strongly affect the velocity inside the vortex core and further analysis on the experimental data are in progress.

References

[1]Billant, P., Chomaz, J. M., and Huerre, P., "Experimental Study of Vortex Breakdown in Swirling Jets," *Journal of Fluid Mechanics*, Vol. 376, 1998, pp. 183–219.

[2]Green, S. I., "Fluid vortices," *Fluid Mechanics and its Applications*, Kluwer Academic Publisher, 1995, pp. 427–470.

[3]Batchelor, G. K., "Axial Flow in Trailing Line Vortices," *Journal of Fluid Mechanics*, Vol. 20, No. 4, 1964, pp. 645–658.

[4]Saffman, P. G. and Moore, D. W., "Axial Flow in Laminar Trailing Vortices," *Proceedings of the Royal Society A*, , No. 333, 1973, pp. 491–508.

[5]Spalart, P. R., "Airplane Trailing Vortices," *Annu. Rev. Fluid Mech.*, Vol. 30, 1998, pp. 107–138.

[6]Chow, J. S., Zilliac, G. G., and Bradshaw, P., "Mean and Turbulence Measurements in the Near Field of a Wingtip Vortex," *AIAA Journal*, Vol. 35, No. 10, 1997, pp. 1561–1567.

[7]Devenport, W. J., Rife, M. C., Lipias, S. I., and Follin, G. J., "The Structure and Development of a Wing-Tip Vortex," *Journal of Fluid Mechanics*, Vol. 312, 1996, pp. 67–106.

[8]Anderson, E. A. and Lawton, T. A., "Correlation Between Vortex Strength and Axial Velocity in a Trailing Vortex," *Journal of Aircraf*, Vol. 40, No. 4, 2003, pp. 699–704.

[9]Zang, W. and Prasad, K., "Performance Evaluation of a Scheimpflug Stereocamera for Particle Image Velocimetry," *Applied Optics*, Vol. 36, No. 33, 1997, pp. 8738–8744.

[10]Lawson, N. J. and Wu, J., "Three-Dimensional Particle Image Velocimetry: Error Analysis of Stereoscopic Techniques," *Meas. Sci. Technol.*, Vol. 8, 1997, pp. 894–900.

[11]Keane, R. D. and Adrian, R. J., "Theory of Cross-Correlation Analysis of PIV Images," *Applied Scientific Research*, Vol. 49, 1992, pp. 191–215.

[12]Giuni, M., Benard, E., and Green, R. B., "Investigation of a Trailing Vortex Near Field by Stereoscopic Particle Image Velocimetry," *49th AIAA Aerospace Sciences Meeting, American Institute of Aeronautics and Astronautics*, Reston, VA (submitted for publication).

[13]Adrian, R. J., "Particle-Imaging Technique for Experimental Fluid Mechanics," *Annual Review Fluid Mechanics*, Vol. 23, 1991, pp. 261–304.

[14]Prasad, A. K., Adrian, R. J., Landreth, C. C., and Offutt, P. W., "Effect of Resoluation on the Speed and Accuracy of Particle Image Velocimetry Interrogation," *Experiments in Fluids*, Vol. 13, 1992, pp. 105–116.

[15]Ramasamy, M., Johnson, B., Huismann, T., and Leishman, J. G., "Digital Particle Image Velocimetry Measurements of Tip Vortex Characteristic Using an Improved Aperiodicity Correction," *Journal of the American Helicopter Society*, Vol. 54, No. 012004, 2009.

[16]M. Raffel, C. Willert, S. W. J. K., *Particle Image Velocimetry: a Practical Guide*, Springer, 2nd ed., 2007.

[17]Giuni, M., Benard, E., and Green, R. B., "Near Field Core Structure of Wing Tip Vortices," *Experimental Fluid Mechanics 2010*, EFM, Liberec, Czech Republic, 2010.

[18]Dacles-Mariani, J., Zilliac, G. G., Chow, J. S., and Bradshaw, P., "Numerical/Experimental study of a wingtip vortex in the near field," *AIAA Journal*, Vol. 33, No. 12, 1997, pp. 1561–1568.